Chiral Recognition Studies: Intra- and Intermolecular $^1H\{^1H\}$-Nuclear Overhauser Effects as Effective Tools in the Study of Bimolecular Complexes

William H. Pirkle* and Shaun R. Selness

School of Chemical Sciences, University of Illinois, Urbana, Illinois 61801

Received June 2, 1994 (Revised Manuscript Received February 24, 1995)

Introduction

The nuclear Overhauser effect (nOe) has been employed successfully in the structural and conformational characterization of compounds such as peptides, steroids, and polynucleotides.[1] Typically, these effects are intramolecular. When observable, *intermolecular* nOes provide information concerning modes of interaction between molecules in solution. Bimolecular systems employed for chiral recognition have been so studied.[2–9] In several cases, the conclusions so reached have been supplemented by crystallographic means.[10] As useful as the solid state data are, crystallization of 1:1 complexes of two components is not always possible. Moreover, the information so obtained is that for the solid state, not the solution state, which more closely mimics the environment in which chromatographic chiral recognition occurs. The observation of both intra- and intermolecular nOes, coupled with chemical shift data, provides insight into the *solution state* behavior of bimolecular systems.

Our interests lie in understanding the interactions responsible for the differential affinities shown toward enantiomers by chiral selectors. The latter may be free in solution or immobilized as chiral stationary phases (CSPs). Although the interactions of enantiomers with a CSP are not rigorously identical to those responsible for chiral recognition in solution, spectroscopic investigations of the latter can advance understanding of the former. Furthermore, spectroscopic studies can be used to assess the validity of chiral recognition models derived solely from chromatographic data.

Recently, we reported the synthesis and evaluation of chiral stationary phases **1** and **2**.[11,12] Originally designed to separate the enantiomers of naproxen, **CSPs 1–3**[13]

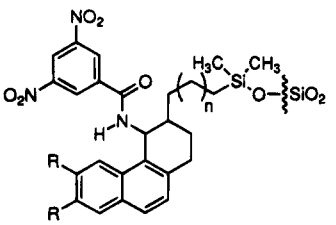

(*R,R*) **CSP 1**; R = H, n = 9
(*S,S*) **CSP 2**; R = H, n = 1
(*S,S*) **CSP 3**; R = CH_3, n = 1

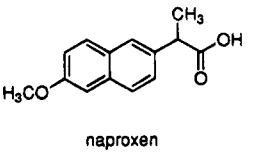

naproxen

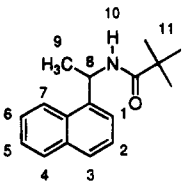

4

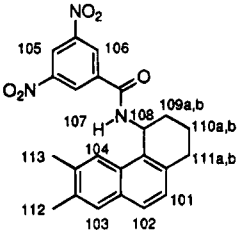

5

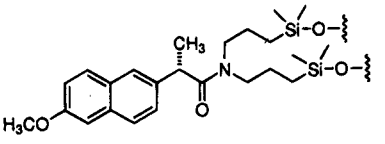

(*S*)-**CSP 4**

are capable of resolving the enantiomers of a large number of compounds, often affording large separation factors, α. Among the readily resolved racemates are amide derivatives of 1-(aryl)alkylamines. For example, **CSP 3** separates the enantiomers of the pivalamide, **4**, of 1-(1-naphthyl)ethylamine with a high degree of selectivity (α = 9.9, 1:2:7 MeOH/2-propanol/*n*-hexane) and affords relatively strong retention of the second eluted enantiomer even in this strong eluent. These properties, coupled with its relatively simple ^1H-NMR spectrum, suggested that **4** would be an appropriate candidate for a spectroscopic investigation of the chiral recognition mechanism employed by **CSP 3** for amides of 1-(aryl)-alkylamines. Compound **5**, a soluble analog of the chiral selector used in **CSP 3**, was prepared and resolved, and a spectroscopic investigation was undertaken on mixtures of (*S*)-**4** and each of the enantiomers of **5**.

From our initial presumption of the intermolecular interactions involved in complexation, a structure proposed for the complex of (*S*)-**4** and (*S*)-**5** is shown in Figure 1. Several perspectives are used to indicate the direction of approach of the analyte to the chiral selector. The electron-rich naphthyl ring of the analyte is expected to participate in a face-to-face $\pi-\pi$ interaction with the electron-deficient 3,5-dinitrobenzamide (DNB) ring of the selector. Additionally, the carboxamide oxygen of the analyte is expected to participate in a hydrogen bond to the acidic 3,5-DNB amide proton of **5**. An edge-to-face $\pi-\pi$ interaction between the naphthyl ring of the analyte

(1) Neuhaus, D.; Williamson, D. *The Nuclear Overhauser Effect in Structural and Conformational Analysis*; VCH Publishers: New York, 1989.
(2) Pirkle, W. H.; Pochapsky, T. C. *J. Am. Chem. Soc.* **1987**, *109*, 5975–5982.
(3) Pirkle, W. H.; Pochapsky, T. C. *J. Am. Chem. Soc.* **1986**, *108*, 5627–5628.
(4) Spisni, A.; Corradini, T.; Marchelli, R.; Dossena, A. *J. Org. Chem.* **1989**, *54*, 684–688.
(5) Galán, A.; de Mendoza, J.; Torion, C.; Bruix, M.; Deslongchamps, G.; Rebek, J. *J. Am..Chem. Soc.* **1991**, *113*, 9424–9425.
(6) Barretta, G. U.; Rosini, C.; Dario, P.; Salvadori, P. *J. Am. Chem. Soc.* **1990**, *112*, 2707–2710.
(7) Sanderson, P. E. J.; Kilburn, J. D.; Still, C. W. *J. Am. Chem. Soc.* **1989**, *111*, 8314–8315.
(8) Pochapsky, T. C.; Stone, P. M. *J. Am. Chem. Soc.* **1990**, *112*, 6714–6715.
(9) Pochapsky, T. C.; Wang, A. P.; Stone, P. M. *J. Am. Chem. Soc.* **1993**, *115*, 11084–11091.
(10) Pirkle, W. H.; Burke, J. A.; Wilson, S. R. *J. Am. Chem. Soc.* **1989**, *111*, 9222–9223.
(11) Pirkle, W. H.; Welch, C. J.; Lamm, B. *J. Org. Chem.* **1992**, *57*, 3854–3860.
(12) Pirkle, W. H.; Welch, C. J. *J. Liq. Chromatogr.* **1992**, *15*, 1947–1955.

(13) Details of the preparation and evaluation of **CSP 3**, first prepared by M. H. Hyun, will be described elsewhere. The synthetic route employed is essentially that used for **CSP 2**.[11,12]

0022-3263/95/1960-3252$09.00/0

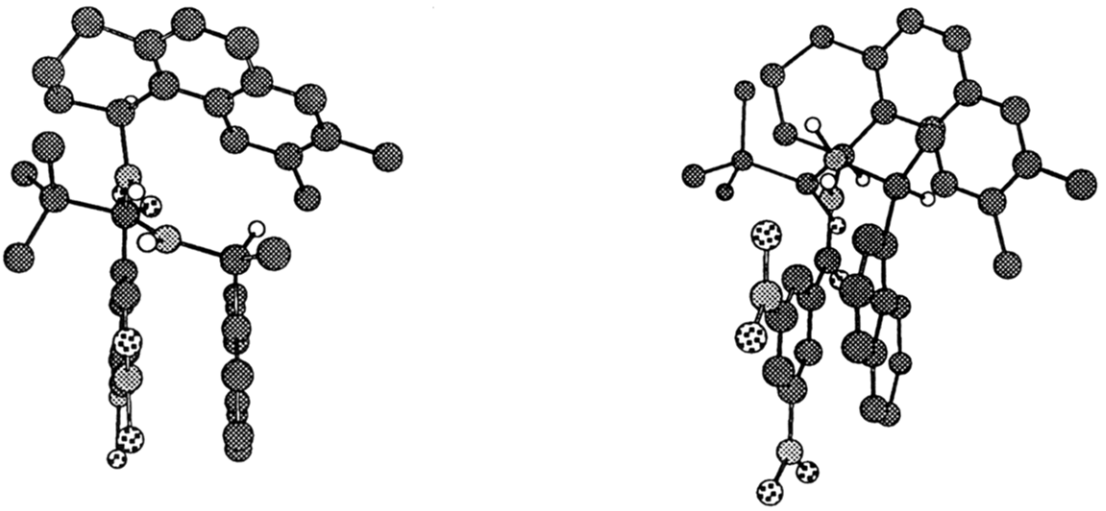

Figure 1. Proposed chiral recognition model for the more stabel (*S,S*)-complex between **4** and **5**. Two views are shown to illustrate the facial approach of the analyte to the selector. The ring and methyl hydrogens have been omitted for clarity.

and the π-cloud of the naphthyl group of **5** is proposed to be the third of the bonding interactions responsible for the observed enantioselectivities. The (*S*)-enantiomer of **4** is believed to be able to undergo these interactions simultaneously with (*S*)-**5** from a low-energy conformation, whereas the (*R*)-enantiomer cannot. The homochiral [i.e. (*S,S*) or (*R,R*)] complex is found to be more stable than the heterochiral diastereomeric complex since (*S,S*)-**CSP 3** preferentially retains (*S*)-**4**.

Results and Discussion

Four $CDCl_3$ samples were prepared for ^{1}H-NMR analysis: (1) nominally 0.025 M in (*S*)-**4**; (2) nominally 0.025 M in (*R*)-**5**; (3) nominally 0.025 M in (*S*)-**4** and 0.025 M in (*S*)-**5**; and (4) nominally 0.025 M in (*S*)-**4** and 0.025 M in (*R*)-**5**. Each sample was degassed and sealed by the freeze−thaw method, and care was taken to ensure that the relative concentrations of each sample remained constant. All spectra were acquired and recorded on a 400 MHz spectrometer. The temperature was maintained at 18 ± 0.3 °C for the duration of the experiments.

^{1}H-NMR Chemical Shift Studies. The (*S,S*)-mixture contains the more stable complex based on the elution behavior of **4** on **CSPs 1−3**. Because the association of the two components in the (*S,R*)-mixture is considerably weaker, consistent with the near absence of induced chemical shift changes, our discussion will focus on the induced chemical shift changes noted for the more stable mixture. When discussing the observed chemical shift changes, one must keep in mind that the measured shifts are a weighted time average of the chemical shifts of all of the species present in solution. That is, the extents to which the chemical shifts of the two components are perturbed in the mixture are dependent on the population(s) of the complex(es) in solution as well as the chemical shifts of each species present. In our discussion, all references to chemical shift differences are relative to the chemical shifts of the individual samples of **4** and **5** at the concentrations employed. Hydrogens 1−11 are in pivalamide **4**; hydrogens 101−113 are in selector **5**.

As shown in Table 1, significant chemical shift differences are observed, relative to the individual analytes, in the mixture of (*S*)-**4** and (*S*)-**5**. Most notably, the 3,5-DNB NH resonance, H107, of (*S*)-**5** is shifted downfield by 1.5 ppm! A series of variable temperature measurements showed that this shift is sensitive to temperature and to the stoichiometry of the mixture. As indicated in Table 2, at lower temperatures and larger (*S*)-**4** :(*S*)-**5** ratios, the shift differences for H107 are quite significant (as large as +3.1 ppm). This suggests that the amide NH is involved in a hydrogen bond and is consistent with the proposal in Figure 1. The resonances of naphthyl hydrogens H104 and H113 are shifted downfield by 0.23

Table 1. Observed ^{1}H Chemical Shifts of Protons in 4 and 5 of the Free Analytes and of the {(*S*)-4, (*S*)-5} and {(*S*)-4, (*R*)-5} Mixtures[a]

proton	free analyte	(*S*)-**4** + (*S*)-**5** (Δδ)	(*S*)-**4** + (*R*)-**5**
H1	7.47	7.25 (−0.22)	7.48
H2	7.50	7.32 (−0.18)	7.46
H3	7.81	7.67 (−0.14)	7.79
H4	7.87	7.70 (−0.17)	7.85
H5	7.50	7.40 (−0.10)	7.49
H6	7.52	7.47 (−0.05)	7.49
H7	8.03	7.70 (−0.33)	8.01
H8	5.89	5.27 (−0.62)	5.85
H9	1.66	1.25 (−0.41)	1.64
H10	5.87	5.70 (−0.17)	5.84
H11	1.18	1.18 (0.00)	1.16
H101	7.17	7.17 (0.00)	7.16
H102	7.64	7.63 (−0.01)	7.63
H103	7.55	7.57 (+0.02)	7.54
H104	7.64	7.87 (+0.23)	7.64
H105	9.01	8.71 (−0.30)	9.02
H106	8.87	8.71 (−0.16)	8.84
H107	6.68	8.20 (+1.48)	6.92
H108	5.95	6.04 (+0.09)	5.95
H111a,b	3.00	3.00 (0.00)	3.00
H112	2.38	2.38 (0.00)	2.37
H113	2.38	2.53 (+0.15)	2.37

[a] All chemical shifts reported in ppm relative to tetramethylsilane in $CDCl_3$ at 18 °C. Nominal concentration for all components is 0.025 M.

Table 2. Variable Temperature Analysis of the More Stable Mixture: Chemical Shifts of H107 at −50, −20, 0, and 10 °C[a]

(*S*)-**4** (mM)/ (*S*)-**5** (mM)	δ (−50 °C)	δ (−20 °C)	δ (0 °C)	δ (10 °C)
2/0	6.77	6.65	6.58	6.56
2/4				
2/8	9.48	8.33	7.61	
2/12	9.79		8.17	8.01
2/16	9.86	9.18	8.48	8.10

[a] All chemical shifts reported in ppm relative to tetramethylsilane in $CDCl_3$.

Table 3. Intramolecular and Intermolecular nOes in the Free and (S,S)-, and (S,R)-Mixtures of 4 and 5 at 18 °C[a]

irradiated proton	free analyte	(S)-4 + (S)-5 (intramolecular)	(S)-4 + (R)-5 (intramolecular)	(S)-4 + (S)-5 (intermolecular)
H1		H2 (8); H10 (3)		
H2		H3 (18)		
H3	H2 (13)		H2 (12); H4 (14)	
H4	H3 (5); H5 (15)		H3 (6); H5 (15)	
H5		H6 (1); H4 (17)		
H6		H5 (5); H7 (7)		H106(1)
H7	H6 (16); H8 (13)		H6 (17); H8 (19)	
H8	H7 (13); H9 (4); H11 (4)	H7 (22)	H7 (15); H9 (3)	H106 (1); H107 (2)
H9	H1 (6); H7 (2); H8, H10 (3)[b]	H1 (5); H7 (2) H8 (5); H10 (3)	H1 (8); H7 (1); H8, H10 (6)[c]	
H10		H1 (7.1)		
H11	H8, H10 (2)[b]	H10 (1.7)	H8, H10 (2)[c]	H101 (1); H106 (2)
H101	H102 (17); H111a,b (4)	H102 (20.0); H111a,b (5)	H102 (16); H111a,b (4)	
H102	H101 (5.4)		H101 (9); H103 (12)	
H103	H102 (11); H112 (7)	H112 (10)		
H104	H106 (1); H108 (9); H113 (3)	H106 (1); H108 (21); H113 (9)	H108 (8); H113 (3)	
H105	H106 (1.0)		H106 (2)	
H106[d]	H105 (3); H107 (5)	H107 (4)	H105 (2); H107 (6)	
H107	H106 (51)	H106 (52)	H106 (53)	H8 (4)
H108	H104 (30)	H104 (26)	H104 (31)	
H111a,b	H101 (18)	H101 (14)	H101 (13)	
H112[e]	H103 (4)	H103 (5)	H103 (3)	
H113[e]	H104 (2)	H104 (4); H106 (1)	H104 (2)	H6 (4)

[a] The nominal concentration of each component is 0.025 M. Percent nOes are shown in parentheses. [b] H8 and H10 are isochronous in the sample of free 4. [c] H8 and H10 are isochronous in the (S,R) mixture of 4 and 5. [d] H105 and H106 are isochronous in the (S,S) mixture of 4 and 5. [e] H112 and H113 are isochronous in the sample of free 5 and in the (S,R) mixture of 4 and 5.

and 0.15 ppm, respectively. The proposed model places these protons in the deshielding region of the naphthyl ring of pivalamide **4** and is thus consistent with the observed downfield shifts. As expected from a face-to-face $\pi-\pi$ interaction, DNB ring protons H105 and H106 experience shielding upon complexation owing to their positioning over the naphthyl ring of (*S*)-**4**. The model also leads one to expect that the methine hydrogen, H8, of (*S*)-**4** will be shielded by the naphthyl π-cloud of (*S*)-**5**. Indeed, a relatively large upfield shift of 0.61 ppm is observed for H8 in the (*S,S*)-mixture! The methyl and amide hydrogens, H9 and H10, experience less shielding than H8 in the (*S,S*) mixture, their respective upfield chemical shift differences being 0.41 and 0.17 ppm. Again, these shifts can be attributed to shielding by the naphthyl π-cloud of (*S*)-**5**. Similarly, all of the aromatic protons of (*S*)-**4** are shifted upfield upon complexation with (*S*)-**5**. Significantly, naphthyl ring proton H7 experiences a 0.33 ppm upfield shift in the (*S,S*)-mixture. This proton is implicated in the proposed edge-to-face $\pi-\pi$ interaction shown in Figure 1 and, in the model, is placed directly over the shielding region of the π-cloud of the naphthyl ring of (*S*)-**5**.

In contrast to the appreciable induced shifts noted in the (*S,S*)-mixture of **4** and **5**, only the DNB amide hydrogen, H107, shows any significant shift in the (*S,R*)-mixture. This downfield shift of 0.24 ppm indicates that this hydrogen is involved in hydrogen bonding, this presumably being the only significant intermolecular interaction between the two components.

Intramolecular ^{1}H{^{1}H}-Nuclear Overhauser Effects. In discussing ^{1}H{^{1}H}-nuclear Overhauser effects, it is important to avoid absolute comparisons of magnitudes owing to the use of different saturation powers for individual resonances. However, it *is* valid to compare relative changes in magnitude upon saturation of a given resonance because the loss of sensitivity is scaled in direct proportion to the actual extent of saturation.[1] As in the discussion of chemical shift differences, our focus will be on the relative changes between the free analytes and the more stable (*S,S*)-mixture. Intramolecular and intermolecular nOe data appear in Table 3.

Changes in the relative intensities of the intramolecular nOes for (*S*)-**4** in the more stable mixture indicate that several conformational changes occur upon complexation. Saturation of methine proton H8 results in enhancements of 13% at naphthyl proton H7, 4% at H9, and 4% at H11 in the noncomplexed analyte, (*S*)-**4**. This enhancement is increased to 22% at H7 in the (*S,S*)-mixture with the absence of any enhancements at H9 and H11. It is likely that this change is due to hydrogen bonding between the carboxamide oxygen of (*S*)-**4** and the amide proton H107 of (*S*)-**5** in the (*S,S*)-mixture. In the complex, this hydrogen bond helps adjust the conformation of pivalamide **4**, placing methine hydrogen H8 closer to the naphthyl proton H7. This provides another dipolar pathway by which H8 can relax, thus diminishing or precluding nOes at H9 and H11. In both the free analyte and the less stable mixture, saturation of aromatic protons H3, H4, and H7 results in intramolecular nOes at H2, H3,H5, and H6,H8, respectively. These nOes are not observed in the more stable mixture. This change is attributed to the ability of heteroatoms such as N and O to participate in dipolar relaxation mechanisms. A $\pi-\pi$ face-to-face interaction between the naphthyl ring of (*S*)-**4** and the DNB ring of (*S*)-**5** would place the nitro groups of the DNB ring in close proximity to the aromatic protons of (*S*)-**4**. This additional relaxation pathway could diminish the importance of the other previously available pathways. Upon saturation of H10 no intramolecular nOes are observed in the free analyte or in the less stable mixture. However, an intramolecular nOe is observed at H1, 7%, in the more stable mixture. This observation might be explained by a change in conformation about the N(**4**)–C8(**4**) bond caused by the hydrogen bond between H107 and OC(**4**). As a result, H10 is placed closer to H1; thus, the observed nOe.

As with (*S*)-**4**, several changes in the relative magnitude of the intramolecular nOes occur for (*S*)-**5** in the (*S,S*)-mixture. For the noncomplexed selector, saturation of naphthyl proton H104 results in enhancements at H106 (1%), H108 (9%), and H113 (3%) in a ratio of 1.0:10.3:3.8. This ratio changes to 1.0:28.7:12.4 in the (*S,S*)-mixture. Speculatively, the reduced relative enhance-

ment at H106 may be a result of rotation of the 3,5-dinitrobenzamide ring away from the naphthyl ring of (*S*)-**5** to better accommodate the face-to-face $\pi-\pi$ interaction shown in Figure 1. The intramolecular enhancements observed for H104 and H106 upon saturation of H113 change in the (*S,S*)-mixture relative to those for free (*S*)-**5**. The ratio changes from 3.7:1 to 3.4:1. This small change is attributed to the introduction of an intermolecular relaxation pathway as evidenced by the observed enhancement at H6.

Of the intramolecular nOes, the most pronounced are those for H106 upon saturation of H107. In both the noncomplexed and the complexed selector, saturation of H107 results in an nOe of >50% at H106. In contrast, saturation of H106 results in relatively small nOes at H107. Assuming that the DNB system of **5** is relatively planar, H106 and H107 should be in close proximity to one another. This is consistent with the large nOe observed for H106 upon saturation of H107. Precedent for large (about 45%) nOes was established by Anet's work on "semiclathrate" compounds.[14] However, the absolute magnitudes (>50%) of the observed nOes are larger than the theoretical maximum positive nOe of 50%. Each of the experiments was repeated three times, resulting in nOes of >50%. Currently, we are at a loss to explain this behavior. The severely diminished nOe observed at H107 upon saturation of H106 is attributed to the exchangable nature of H107.[1]

Intermolecular $^1H\{^1H\}$-Nuclear Overhauser Effects. The observation of several small but reproducible intermolecular nOes in the more stable (*S,S*)-mixture provides strong spectroscopic evidence for the proposed chiral recognition mechanism. These intermolecular nOes are shown in Table 3. All observed intermolecular nOes were reproduced three times to within 0.2% of each other. Upon saturation of the *tert*-butyl resonance, H11 of (*S*)-**4**, an intermolecular nOe is observed for DNB ring proton H106. This suggests that the *tert*-butyl group spends a significant amount of time near the DNB ring; the proposed mechanism accounts for this proximity. The intermolecular nOe observed for H6 upon saturation of H113 is supportive of a mechanism in which the naphthyl ring of (*S*)-**4** is oriented in an edge-to-face fashion relative to the naphthyl ring of (*S*)-**5**. Saturation of the methine proton, H8, of (*S*)-**4** results in nOes at DNB proton, H106, and DNB amide proton, H107, of (*S*)-**5**. With reference to Figure 1, the proposed mechanism does predict that the methine proton should be in proximity to H107 and H106. A large reciprocal nOe at H8 is observed upon saturation of H107, again establishing their proximity. Finally, saturation of naphthyl ring proton, H6, of (*S*)-**4** results in an nOe at DNB proton, H106. Though difficult to depict in two dimensions, inspection of space-filling models reveals that, in the proposed structure, H6 is directly above H106.

Conclusion

Spectroscopic observations of small, reproducible *intermolecular* nOes, along with chemical shift changes that occur when (*S*)-**4** interacts with (*S*)-**5**, provide support for a chromatographically derived chiral recognition model which accounts for the ability of **CSP 3** to differentiate between the enantiomers of analytes such as **4**. This study illustrates the utility of NMR data in conjunction with chromatographic data for establishing the structure of transient bimolecular complexes.

(14) Anet, F. A.; Bourn, J. R.; Carter, P.; Winstein, S. *J. Am. Chem. Soc.* **1965**, *87*, 5249–5250.

Experimental Section

General. All reagents used were of pharmaceutical or reagent grade, and solvents used in spectroscopic studies were of spectrophotometric grade. Except where noted, all ^{1}H-NMR spectra were recorded on a 400 MHz FT-NMR operating at 400 MHz in the ^{2}H lock mode. Chemical shifts are reported in parts per million (ppm) relative to TMS, and coupling constants are reported in hertz. All ^{13}C-NMR spectra were recorded on a 400 MHz FT-NMR operating at 100 MHz in the ^{2}H lock mode. Chemical shifts are reported in ppm relative to $CDCl_3$ (77 ppm). Melting points are uncorrected. Elemental analyses were performed by T. McCarthy and associates of the University of Illinois microanalytical service. Optical rotations were recorded using a digital polarimeter equipped with a 1 dm cell operating at 589 nm (sodium D line).

(*S*)-1-[(2,2-Dimethylpropanoyl)amino]-1-naphthylethane (4). A CH_2Cl_2 solution (10 mL) of 0.50 g (2.9 mmol) of (*S*)-1-(1-naphthyl)ethylamine (purchased from Aldrich) and 0.8 mL (5.8 mmol) of Et_3N was cooled to 0 °C and was treated with 0.4 mL (3.2 mmol) of pivaloyl chloride. The solution was stirred for 9 h at room temperature. The reaction mixture was diluted with 100 mL of CH_2Cl_2 and was washed (3 × 50 mL) with 1 M HCl and 100 mL of water. The organic layer was dried over anhydrous $MgSO_4$, and the solvent was removed to leave 0.70 g of a white solid. The solid was chromatographed on silica (5% EtOAc/CH_2Cl_2) to afford 0.65 g (87%) of a white crystalline solid: mp = 139–140 °C; enantiomeric purity of the sample established by chiral HPLC on **CSP 2** (%ee = 99%); ^{1}H NMR (400 MHz, $CDCl_3$) δ 1.18 (s, 1H), 1.66 (d, J = 6.5 Hz, 1H), 5.85 (bs, 1H), 5.89 (m, J = 6.5 Hz, 1H), 7.44–7.54 (m, 4H), 7.81 (d, J = 7.9 Hz, 1H), 7.87 (d, J = 7.2 Hz, 1H), 8.03 (d, J = 8.6 Hz, 1H); ^{13}C NMR (100 MHz, $CDCl_3$) δ 20.47, 27.49, 38.68, 44.62, 122.47, 123.49, 125.12, 125.88, 126.47, 128.38, 128.71, 131.20, 133.90, 138.27, 177.40; $[\alpha]_D$ −33.4 (10 mg/mL THF). Anal. Calcd for $C_{17}H_{21}NO$: C, 79.96; H, 8.29; N, 5.49. Found: C, 79.95; H, 8.28; N, 5.51.

3-[2-(5,6-Dimethylnaphthoyl)]propionic Acid. A 1 L round-bottom flask was charged with 150 mL of CH_2Cl_2, 100 mL of CH_3NO_2, a magnetic stir bar, 11.65 g (116 mmol) of succinic anhydride, and 51.21 g (384 mmol) of $AlCl_3$. The flask was immersed in an ice bath, and a solution of 20.00 g (128 mmol) of 2,3-dimethylnaphthalene in 100 mL of CH_2Cl_2 was added dropwise to the stirred mixture over a 1 h period. The dark solution was stirred and allowed to warm to room temperature over a period of 20 h. The reaction was carefully quenched over ice/concd HCl. The precipitate was removed by filtration and was washed with CH_2Cl_2. The brown solid was recrystallized from EtOAc to afford 16.7 g (56%) of pale brown crystals: mp 184–185 °C; ^{1}H NMR (400 MHz, $CDCl_3$) δ 2.46 (bs, 6H), 2.87 (t, J = 6.6 Hz, 2H), 3.46 (t, J = 6.6 Hz, 2H), 7.63 (s, 1H), 7.71 (s, 1H), 7.77 (d, J = 8.6 Hz, 1H), 7.95 (d, J = 8.6 Hz, 1H), 8.41 (s, 1H); ^{13}C NMR (100 MHz, $CDCl_3$) δ 20.18, 20.45, 27.94, 33.20, 122.94, 123.08, 127.32, 128.98, 131.31, 132.93, 134.69, 136.73, 138.94, 176.97, 205.03. Anal. Calcd for $C_{16}H_{16}O_3$: C, 74.98; H, 6.29. Found: C, 74.97; H, 6.30.

4-[2-(5,6-Dimethylnaphthyl)]butyric Acid. A 500 mL Parr bottle was charged with 3.0 g (11.7 mmol) of **6**, 1.5 g of 5% Pd/C, and 100 mL of THF. The mixture was subjected to a H_2 pressure of 50 psi and was rocked gently for 24 h (final pressure = 40 psi). The suspension was filtered through Celite and the filtrate washed with 50 mL of water. The organic layer was dried over anhydrous $MgSO_4$, and the solvent was removed to leave 2.8 g (100%) of a white crystalline solid: mp 140–141 °C; ^{1}H NMR (400 MHz, $CDCl_3$) δ 2.04 (m, 2H), 2.40 (t, J = 7.7, 2H), 2.42 (bs, 6H), 2.81 (t, J = 7.8, 2H), 7.22 (d, J = 8.1, 1H), 7.51 (s, 1H), 7.54 (s, 1H), 7.56 (s, 1H), 7.65 (d, J = 8.1, 1H); ^{13}C NMR (100 MHz, $CDCl_3$) δ 20.12, 20.21, 26.08, 33.15, 35.08, 125.63, 126.29, 126.92, 126.98, 127.06, 130.95, 132.43, 134.84, 135.62, 137.63, 179.22. Anal. Calcd for $C_{16}H_{18}O_2$: C, 79.31; H, 7.49. Found: C, 79.04; 7.38.

6,7-Dimethyl-4-oxo-1,2,3,4-tetrahydrophenanthrene. A 250 mL round-bottom flask was charged with 2.8 g (11.6 mmol)

of **7**, 21 mL (7 mL/g of substrate) of methanesulfonic acid, and a magnetic stir bar. The solution was stirred for 1.5 h at room temperature, and the reaction was quenched over ice. The aqueous mixture was extracted (3 × 100 mL) with Et_2O. The combined organic extracts were washed (2 × 100 mL) with water and were dried over anhydrous $MgSO_4$. The solvent was removed to leave 2.5 g of a pale yellow solid. The solid was chromatographed on silica (80% CH_2Cl_2/hexane) to afford 2.2 g (85%) of a white crystalline solid: mp 110−112 °C; ^{1}H NMR (200 MHz, $CDCl_3$) δ 2.11 (m, 2H), 2.38 (s, 3H), 2.42 (s, 3H), 2.72 (t, J = 7.7, 2H), 3.02 (t, J = 7.7, 2H), 7.20 (d, J = 8.2, 1H), 7.51 (s, 1H), 7.79 (d, J = 8.1, 1H), 9.18 (s, 1H); ^{13}C NMR (100 MHz, $CDCl_3$) δ 19.80, 20.74, 23.02, 31.49, 41.07, 125.89, 126.49, 127.77, 130.07, 131.73, 133.28, 135.22, 138.80, 145.85, 200.54. Anal. Calcd for $C_{16}H_{16}O$: C, 85.68; H, 7.19. Found: C, 85.73; H, 7.27.

6,7-Dimethyl-4-(3,5-dinitrobenzamido)-1,2,3,4-tetrahydrophenanthrene (5). To a solution of 1.2 g (5.35 mmol) of 6,7-dimethyl-4-oxo-1,2,3,4-tetrahydrophenanthrene in 50 mL of 2-propanol was added 2.4 g (37.4 mmol) of $NaCNBH_3$ and 12 g (161 mmol) of NH_4OAc. The mixture was stirred and warmed to reflux for 22 h. The reaction was quenched by the addition of 50 mL of 2 M NaOH. The mixture was extracted (3 × 75 mL) with CH_2Cl_2. The combined extracts were washed with 100 mL of water and 100 mL of brine. The organic layer was dried over anhydrous K_2CO_3, and the solvent was removed to leave 1.0 g of a pale yellow solid. The solid was dissolved in 40 mL of THF, and 2.1 g (8.9 mmol) of 3,5-dinitrobenzoyl chloride and 0.5 g (8.9 mmol) of propylene oxide were added. The solution was allowed to stir for 4 h at room temperature. The solution was diluted with 200 mL of Et_2O and was washed (3 × 100 mL) with 2 M NaOH and 200 mL of brine. The organic layer was dried over anhydrous K_2CO_3, and the solvent was removed to leave 1.5 g of a yellow solid. The solid was chromatographed on silica (10% EtOAc/CH_2Cl_2) to afford 1.4 g (64% from the ketone, **8**) of a yellow crystalline solid: ^{1}H NMR (400 MHz, $CDCl_3$) δ 1.82−2.06 (m, 3H), 2.25 (m, J = 8.0 Hz, 1H), 2.38 (bs, 6H), 3.00 (m, 2H), 5.95 (m, 1H), 6.68 (d, J = 7.4 Hz, 1H), 7.17 (d, J = 8.5 Hz, 1H), 7.55 (s,1H), 7.64 (s, 1H), 7.64 (d, J = 8.5 Hz, 1H), 8.87 (d, J = 2.1 Hz, 2H), 9.08 (t, J = 2.1 Hz, 1H); ^{13}C NMR (100 MHz, $CDCl_3$) δ 18.16, 19.89, 20.83, 29.07, 29.83, 44.99, 120.95, 122.11, 127.03, 127.13, 127.76, 127.82, 128.35, 130.59, 131.38, 135.13, 161.39. Anal. Calcd for $C_{23}H_{21}N_3O_5$: C, 65.86; H, 5.05; N, 10.02. Found: C, 65.67; H, 4.94; N, 10.13.

Resolution of Racemic 6,7-Dimethyl-4-(3,5-dinitrobenzamido)-1,2,3,4-tetrahydrophenanthrene (5). The enantiomers of **5** were resolved on a preparative di-*n*-propyl linked CSP (**CSP 4**) derived from (*S*)-(−)-2-[2-(6-methoxynaphthyl)]propionic acid. The preparative separation (MPLC) was performed using a Crane MPLC pump and a Linear UVis 200 variable wavelength detector (254 nm). A single run (15% THF/hexane) was performed on 1.5 g of racemic **5** to afford 700 mg of the more retained enantiomer, (*R*)-**5**, $[\alpha]_D$ +36.4 (10 mg/mL THF), and 730 mg of the less retained enantiomer, (*S*)-**5**, $[\alpha]_D$ −35.9 (10 mg/mL THF). The order of elution is inferred from the behavior of amide derivatives of 2-[2-(6-methoxynaphthyl)]propionic acid on (3*S*,4*S*)-**CSP 3**. The (*S*)-enantiomer of 2-[2-(6-methoxynaphthyl)]propionic acid is the less retained enantiomer on (3*S*,4*S*)-**CSP 3**. Assuming that the configuration at the 3,5-dinitrobenzamide position (the 4-position) of **CSP 3** is the critical factor in determining the enantioselectivity and applying the concept of reciprocity, (*R*)-**5** should be the more highly retained enantiomer on **CSP 4**. The enantiomeric purity of each sample was determined by chiral HPLC.

^{1}H-NMR Studies. All $CDCl_3$ used for chemical shift experiments and nOe experiments was passed through activated basic alumina to remove traces of DCl and HCl. Samples of **2** and **3** were dried in a vacuum desiccator, dissolved in purified $CDCl_3$, transferred to suitable 5 mm NMR tubes, exhaustively degassed by the freeze−thaw method, and sealed under vacuum. Samples prepared in this way showed no signs of decomposition. The resonances of exchangeable amide protons did not diminish in intensity, nor did they drift from their original positions over long periods of time. Observable concentration of the samples did occur during the freeze−thaw process. However, care was taken to subject each sample to the same conditions so that relative concentrations remained constant.

Chemical Shift Studies. All spectra for the chemical shift studies were acquired at a probe temperature of 18 °C and were acquired using a 90° pulse width and an appropriate delay on a 400 MHz FT-NMR (number of transients = 16, acquisition time = 4.0 s).

^{1}H{^{1}H}-Nuclear Overhauser Effect Measurements. Nuclear Overhauser effect experiments were performed using a Cyclenoe macro on a 400 MHz FT-NMR. Nuclear Overhauser enhancements were obtained by saturation of the desired resonance during a preacquisition time (set to 5 times the longest T_1 of the sample). The difference spectrum was obtained directly from the macro. Percent nOes were calculated by setting the integral for the saturated resonance equal to −100 (inverted signal). The percent nOes are reported as percentages of this inverted signal. The decoupler power was optimized for each saturated resonance to achieve maximum saturation with maximum selectivity. For these reasons, direct comparisons from experiment to experiment are not valid. A reference spectrum was obtained along with each enhanced spectrum. A total of 32 transients were collected at each irradiation frequency per experiment.

Acknowledgment. Financial support from the National Science Foundation, Eli Lilly, and the U.S. Department of Education is gratefully acknowledged. We thank EM Science for their generous donation of the chromatographic solvents employed in this study.

Supplementary Material Available: Copies of ^{1}H NMR spectra of (*S*)-4, (*R*)-5, ((*S*)-4 and (*R*)-5), and ((*S*)-4 and (*S*)-5) (4 pages). This material is contained in libraries on microfiche, immediately follows this article in the microfilm version of the journal, and can be ordered from the ACS; see any current masthead page for ordering information.

JO940923A